Journal of Materials and Environmental Science
ISSN : 2028-2508
CODEN : JMESCN

J. Mater. Environ. Sci., 2021, Volume 12, Issue 12, Page 1320-1331

http://www.jmaterenvironsci.com

A comprehensive study on the welded joints appearance in GMAW

H.R. Ghazvinloo[1,*], A. Honarbakhsh-Raouf[1], N. Shadfar[2]

[1] *Department of Materials Engineering, Semnan University, Semnan, Iran.*

[2] *Department of Mechanical Engineering, Semnan University, Semnan, Iran.*

[*] *Corresponding author: Hamid.Ghazvinloo@gmail.com.*

Received 08 Sept 2021,
Revised 27 Oct 2021,
Accepted 28 Oct 2021

Keywords
- ✓ *GMAW,*
- ✓ *Appearance,*
- ✓ *Welded joint,*
- ✓ *Welding parameters,*
- ✓ *AA6061,*
- ✓ *C-80,*
- ✓ *CK45*

Hamid.Ghazvinloo@gmail.com
Phone: +989101410684

Abstract

Gas metal arc welding (GMAW) is one of the most famous joining methods which uses heat from the electric arc to melt the tip of the filler metal and the surface of the base materials and bond the workpieces together. This process is usually divided into two sub methods, including MIG (Metal Inert Gas) and MAG (Metal Active Gas) which are used to weld the aluminum alloys and steels, respectively. The appearance of welding joints is an important factor to evaluate the weld quality. Arc voltage (V), welding current (I), and welding speed (S) are three principal variables of GMAW process that can strongly affects the appearance of a welding joint. The aim of this article is to comprehensively study the appearance of welded joints in GMAW process. For this purpose and due to high industrial importance, AA6061 aluminum alloy, C-80 steel, and CK45 steel were chosen as the base materials. After finishing the welding operations, the top surface and cross-section of all welded joints were completely inspected by the visual testing (VT) procedure, the weld defects were detected, and bead penetration was measured for all welded joints. The results indicated various weld defects and varied bead penetrations in the different base materials.

1. Introduction

Welding is an important process commonly used to join the different materials together [1]. Numerous metallic materials can be joined using various welding methods, including FSW, FSSW, USW, GTAW, LBW, GMAW, and ASW. All of these methods have different advantages and disadvantages in terms of cost, appropriateness, labor, training, efficiency, time, temperature, and simplicity [2–7]. GMAW is an important joining process widely used in metal fabrication industries [8]. It is also known as MIG/MAG welding where MIG (Metal Inert Gas) refers to the use of an inert gas (i.e. argon and helium) while MAG (Metal Active Gas) involves the use of an active gas (i.e. carbon dioxide and oxygen) [9]. This process is versatile, since it can be applied for all welding positions; it can easily be integrated into the robotized production canters. These advantages have motivated many researchers to study GMAW process in detail [10]. The robotic welding process has more advantages than the conventional manual process because the quality of the weld is more consistent, the process speed is higher as compared with the manual process. Moreover, we get less wastes and reduced costs [11]. In the GMAW process, heat is generated by an electric arc and incorporates a continuously fed consumable electrode shielded by an externally supplied gas [12]. The commonly used shielding gases in the GMAW process are carbon dioxide

(CO_2), argon (Ar), and their combinations. The application of these shielding gases may provide good protection of the molten droplets and weld pool. However, they also affect the formation of the welding arc, arc stability, and metal transfer [13]. This process involves large number of interdependent variables that can affect product quality, productivity and cost effectiveness. The appearance of welding joints is an important factor to evaluate the weld quality so in this paper, we make an attempt to study the effects of GMAW variables on the appearance of welding joints in various base materials.

2. Methodology

Due to high importance in industry, plates of (i) AA6061 aluminum alloy with 2.35 mm thickness (ii) C-80 steel with 4 mm thickness, and (iii) CK45 steel with 2.5 mm thickness were chosen as base materials. The chemical composition of the base materials was as follows (wt.%): AA6061 aluminum alloy: Al-Base, 0.54 Fe, 0.12 Mn, 0.65 Si, 0.26 Cu, 0.98 Mg, 0.32 Cr, 0.20 Zn, 0.11 Ti, C-80 steel: 0.81 C, 0.22 Si, 0.65 Mn, 0.01 P, 0.01 S, CK45 steel: 0.45 C, 0.22 Si, 0.55 Mn, 0.002 P, 0.013 S. The GMAW welding operations were performed by means of a SOS Model DR Series ARK ROBO 1500 welding robot with a working capacity of 0-600 A and 0-50 V ranges. The GMAW welding robot and its apparatus are illustrated in Fig. 1. 100% argon and ER5356 (AWS A5.10 standard) with 1 mm diameter were used as shielding gas and filler metal to weld the AA6061 aluminum alloy. Correspondingly, shielding gas of 100% CO_2 and ER70S-6 (AWS A5.18 standard) with 1.2 mm and 1 mm diameter were used to weld the C-80 and CK45 steels, respectively. The chemical compositions of the filler metals are listed in Table 1.

Table 1. The chemical composition of the filler metals used in experiments.

ER5356	Mg	Mn	Si	Fe	Cr	Ti	Zn	Cu	Al
wt. (%)	5.00	0.13	0.25	0.40	0.13	0.13	0.10	0.10	Balance
ER70S-6	C	Mn	Si	Cu	S	P			
wt. (%)	0.11	1.63	0.95	0.50	0.025	0.035			

Three independent variables in the experiments were arc voltage (V), welding current (I), and welding speed (S), whereas the other parameters were fixed during experiments. Depending on the type of base material, three different values were chosen for each variable according to Table 2, and a same combination of variables according to Table 3 was used for GMAW welding operations. The welding system applied in this study was single-pass, in a flat position, and performed on square butt joints. To prevent welding distortion, experimental test plates were fixed in the fixture jig before the welding process. Having finished the welding process, first, a complete visual inspection was performed on the top surface of GMAW samples at room temperature, then the cross-section surface of GMAW samples was machined, removed from each impurity, polished, and etched using 2% nital for further investigations.

Table 2. Three different values chosen for welding variables.

Base material	Arc voltage, V (V_1, V_2, V_3)	Welding current, A (I_1, I_2, I_3)	Welding speed, cm/min (S_1, S_2, S_3)
AA6061	20, 23, 26	110, 130, 150	50, 60, 70
C-80, CK45	23, 25, 27	100, 110, 120	42, 62, 82

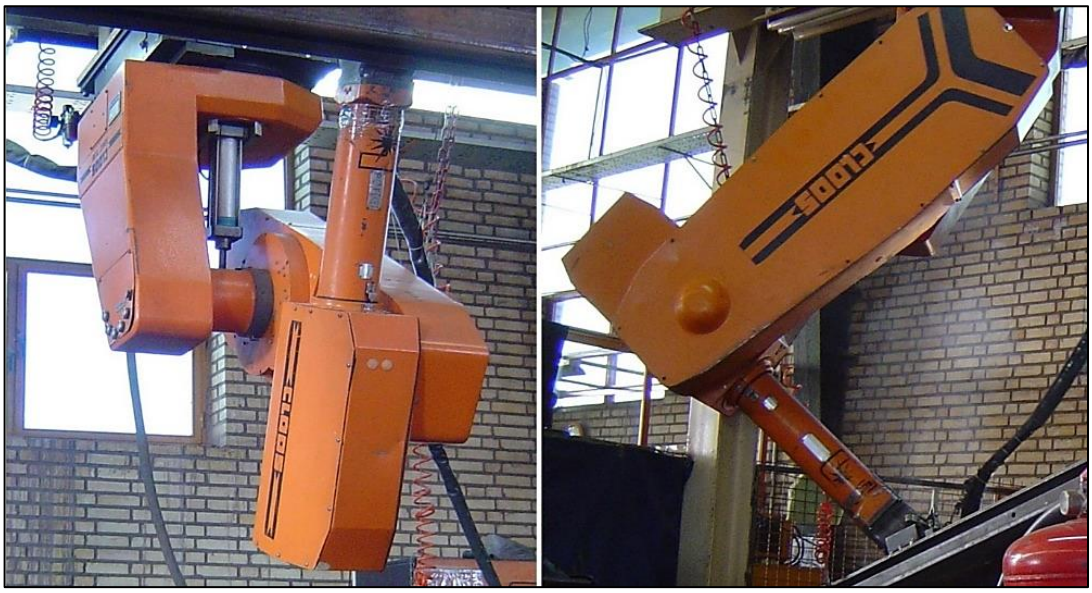

Figure 1. The GMAW welding robot and its apparatus used in experiments.

Table 3. The combination of welding variables in this study

No	I (A)	V (V)	S (cm/min)	No	I (A)	V (V)	S (cm/min)	No	I (A)	V (V)	S (cm/min)
1			S_1	10			S_1	19			S_1
2		V_1	S_2	11		V_1	S_2	20		V_1	S_2
3			S_3	12			S_3	21			S_3
4			S_1	13			S_1	22			S_1
5	I_1	V_2	S_2	14	I_2	V_2	S_2	23	I_3	V_2	S_2
6			S_3	15			S_3	24			S_3
7			S_1	16			S_1	25			S_1
8		V_3	S_2	17		V_3	S_2	26		V_3	S_2
9			S_3	18			S_3	27			S_3

3. Results and Discussion

For each base material in this study, 27 welding joints were produced at different values of I, V, and S according to Tables 2 and 3. Then the top surface and cross-section of welded joints were completely inspected by the visual test procedure at room temperature. All results of this study are shown in Figs. 2-6. Figs. 2 and 3 show the top surface and cross-section of the welded joints for AA6061 aluminum alloy. The weld metal zone, base metal zone, and weld ripples are observed in Figs. 2-1, -14. In addition to these zones, fusion lines are also observed in Fig. 3. According to the Figs. 2 and 3, welding of AA6061 aluminum alloy by GMAW process at different values of I, V, and S can lead to various defects such as

(i) Spatter,
(ii) Undercut,
(iii) Overlap,
(iv) Porosity,
(v) Excessive penetration,
(vi) Irregular surface appearance,
(vii) Rough surface appearance,
(viii) Waviness of bead

As seen in Fig. 2, the top surface of welded joints can provide a clearer view of the spatter, irregular surface appearance, rough surface appearance, and waviness of bead, whereas, undercut, overlap, deep porosity, and excessive penetration can be more obviously detected in cross-section profiles shown in Fig. 3. From observations, spatter is formed on the top surface of a large number of welded joints, however, at a moderate welding current of 130 A, the spatter formation is relatively lower. The spatter defect is defined as droplets of molten material that are formed near the welding arc during the welding process, and ejected from the weld puddle. The ejection of molten material has numerous causes. A prominent cause of ejection is the arc failing to start [14,15]. Spatter is often a result of parameters that have not been properly optimized [15-17]. Spatter can lead to low-quality welds and make the welding area messy. Furthermore, spatter wastes consuming materials in a welding process. Removing spatter from the workpieces surface increases the production time and cost. The undercut is observed in Figs. 2-10, -19, -20, 3-a, -d. The undercut defect is associated with either improper welding techniques or excessive welding currents, or both. This defect is generally located parallel to junction of weld metal and base metal at the toe or root of the weld [18-20] that produces stress concentration and lowers the strength of the weld. The stress concentration factor of an undercut is due to the reinforcement angle, undercut width, undercut depth and undercut root radius [21]. The overlap is observed in Figs. 3-a, -b, -d, -g. The overlap defect occurs when molten metal flows over the surface of the base material and then cools without fusing with the base material. A typical cause of overlap is the supply of too much weld metal due to low welding speed [22]. According to Fig. 3, deep porosity is seen on the cross-section of most welded joints such as Figs. 3-a, -b, -e, -f, -g. The porosity defect refers to cavity-type discontinuities or pores formed by gas entrapment during the solidification of molten weld metal. In arc-welding, it is caused by dissolved gases that are usually present in a molten weld metal. If the dissolved gases are present in amounts greater than their solubility limits, the excess is forced out of the solution in the form of bubble or gas pockets as the weld metal solidifies [23]. Porosity reduces the sectional area under load [24] and the main consequence of porosity in the weld metal is the lowered strength of the joint [25-28]. The total range of bead penetration for AA6061 Aluminum alloy was between 2.310 mm and 3.202 mm with an average bead penetration of 2.814 mm. Other than the joint produced at 110 A, 20 V, and 70 cm/min with a bead penetration of 2.310 mm in which the bead had a minor incomplete penetration, an excessive penetration was observed in all other joints. The maximum over-penetration for AA6061 aluminum alloy in this study was 0.852 mm. Excessive penetration occurs when the weld metal melts through the base metal and hangs underneath the weld. It most often results from too much heat [29]. Excessive root penetration or sometimes referred to as over-penetration in welding is a root contour that extends beyond the acceptable limits and appears as a bead that is high on the underside of the plate or on the inside of the weld [30]. A welded joint with a regular surface appearance is observed at 110 A, 23 V, and 50 cm/min. The welding joint produced in this condition seems to have the most desirable surface appearance with a high quality. Conversely, a welded joint with an irregular surface appearance can be observed in Fig. 2-21, produced at 150 A, 20 V, and 70 cm/min. At an irregular surface, the weld ripples are arranged in an irregular, non-uniform, and messy manner. A moderate welding current of 130 A compared to 110 and 150 A caused the maximum number of welding joints having a rough surface appearance. The welded joints with a rough surface appearance can be observed in Figs. 2-9, -15, -16, -17. In a rough surface appearance, the weld ripples appear too thick, coarse and raised. This rough surface collects deposits thereby increasing the risk of corrosion and product contamination.

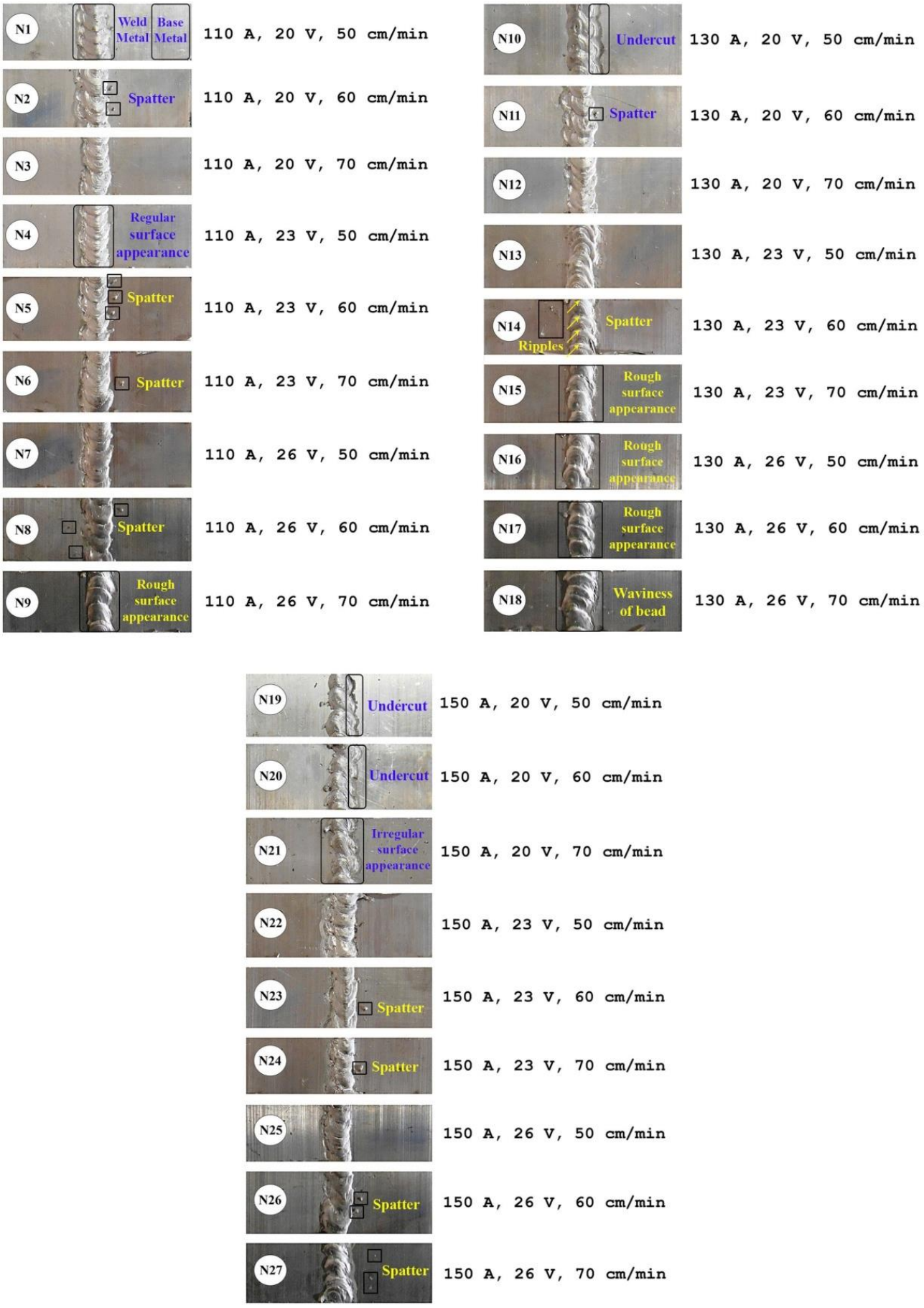

Figure 2. Top surface of welded joints in AA6061 aluminum alloy.

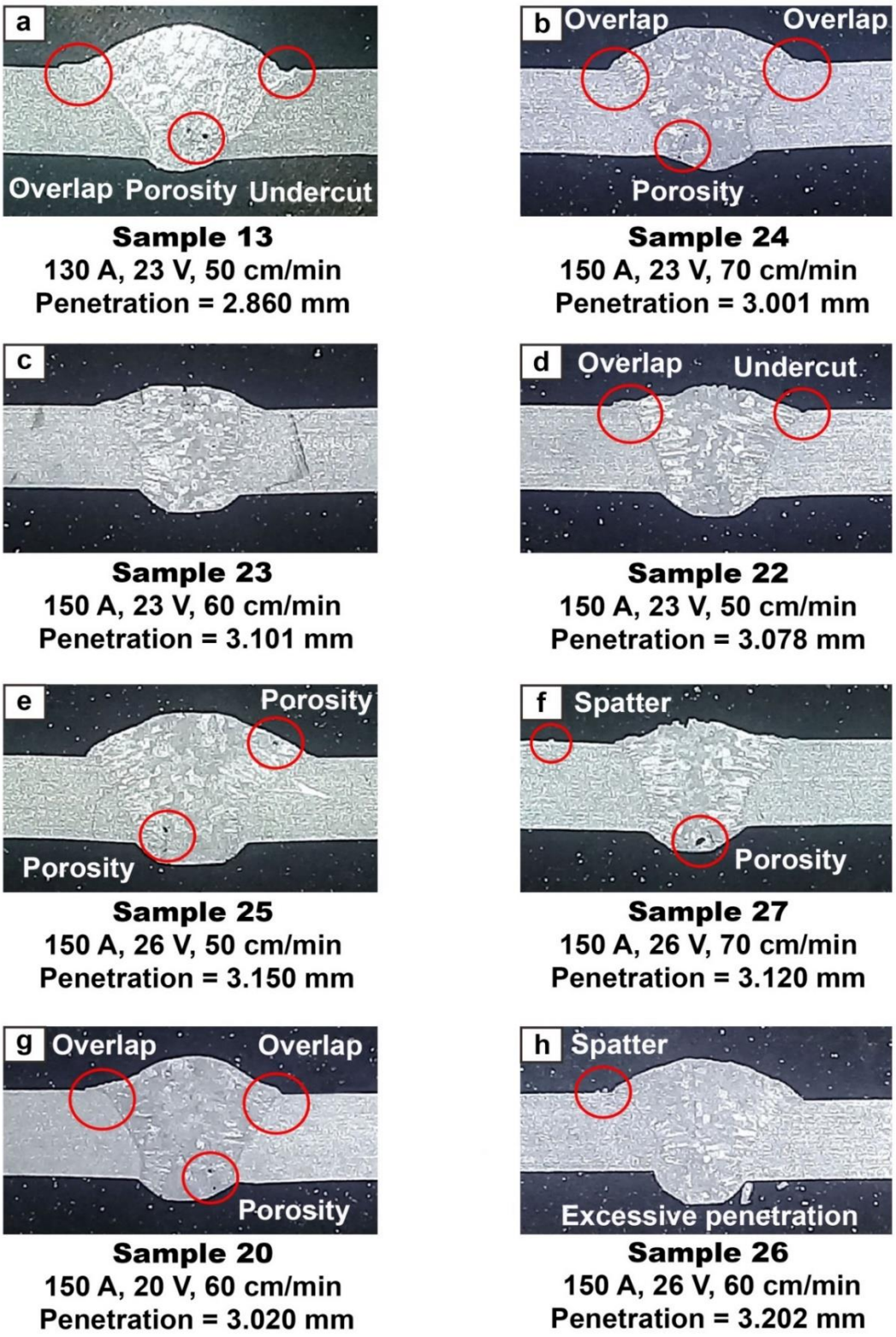

Figure 3. Cross-section of welded joints in AA6061 aluminum alloy.

Manufacturing methods that result in rough surfaces should generally be avoided [31]. The welding joint produced at 130 A, 26 V, and 70 cm/min (Fig. 2-18) had the defect of waviness of bead. In waviness of bead, the welding path is non-linear with a wavy pattern. In this case, weld metal does not completely cover the seam between the workpieces. Figs. 4 and 5 show the top surface and cross-section of the welded joints for C-80 steel. The weld metal zone, base metal

zone, heat-affected zone (HAZ), and fusion lines are clearly observed in these figures. Heat-affected zone is the region between the base metal and weld metal where has the lowest toughness in a welding joint, and fusion lines are boundaries between the weld metal and HAZ in a fusion-welding process. According to Fig. 4, spatter defect is formed on the top surface of most welded joints in C-80 steel. The total range of bead penetration in C-80 steel was between 2.72 mm and 3.27 mm with an average bead penetration of 3.03 mm. All welding joints produced in C-80 steel contained an incomplete penetration. Lack of penetration (LOP) occurs when the weld bead does not penetrate the entire thickness of the base plates [32]. As the weld depth is not sufficient in this condition, this zone will be highly stressed and can fail easily [33]. The joints with complete penetration are widely used for many welding structures where the high weld strength is required [34].

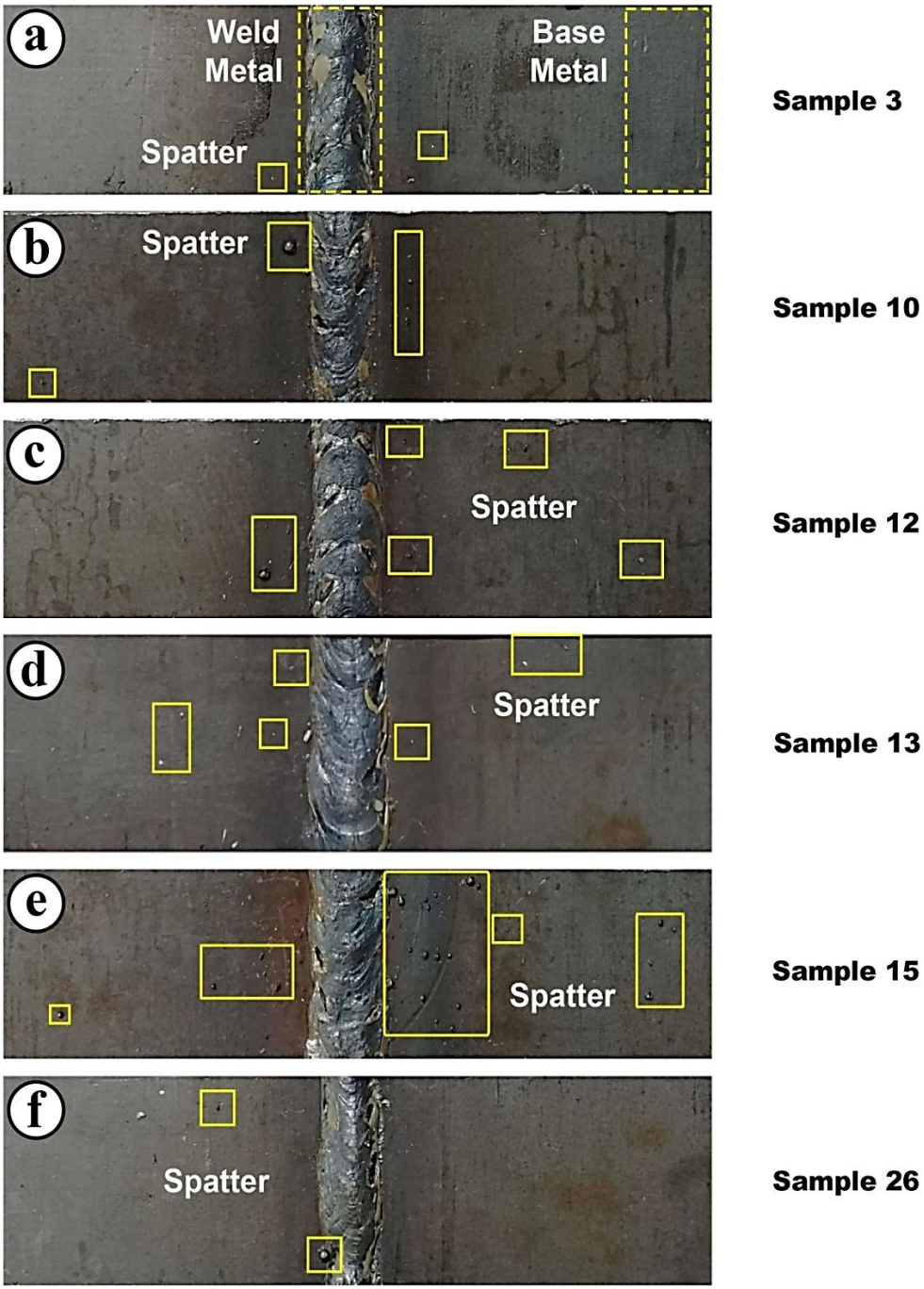

Figure 4. Top surface of welded joints in C-80 steel.

Fig. 6 shows the cross-section of the welded joints in CK45 steel. The weld metal zone, base metal zone, HAZ, and fusion lines are clearly observed in this figure. As seen in Figs. 6-a, -b, -c, welding of CK45 steel by GMAW process at different values of I, V, and S leads to spatter defect and excessive penetration. From observations, spatter defect is more likely to occur at a low or moderate welding current in this study (100 A and 110 A), and no spatter is observed at a welding current of 120 A. The total range of bead penetration in CK45 steel was between 2.437 mm and 3.320 mm with an average bead penetration of 2.937 mm. Other than the joint produced at 100 A, 23 V, and 82 cm/min with a bead penetration of 2.437 mm in which the bead had a minor incomplete penetration, an excessive penetration was observed in all other joints. The maximum over-penetration for CK45 steel in this study was 0.82 mm. Our other studies on welding CK45 carbon steel by GMAW process have been published in previous literatures [35-38].

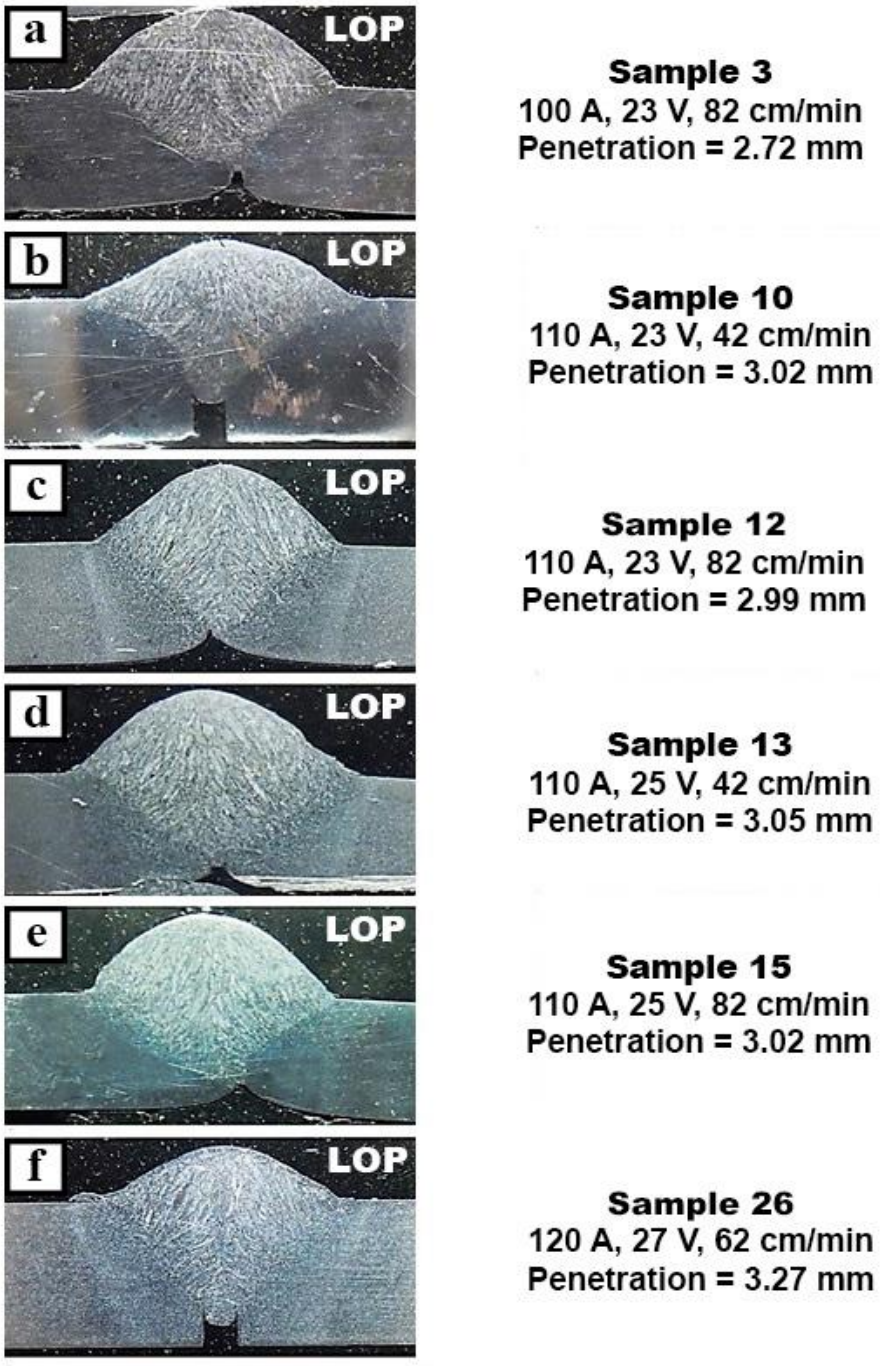

Figure 5. Cross-section of welded joints in C-80 steel.

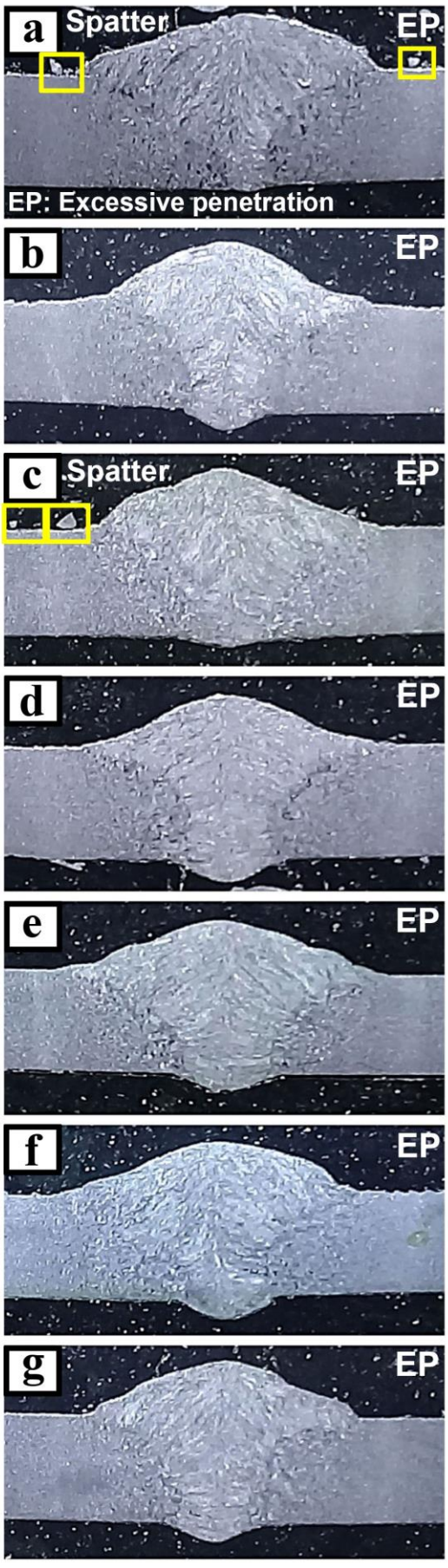

Figure 6. Cross-section of welded joints in CK45 steel.

Conclusion

Welding of AA6061 aluminum alloy by GMAW process at different values of I, V, and S led to various defects such as (i) spatter, (ii) undercut, (iii) overlap, (iv) porosity, (v) excessive penetration, (vi) irregular surface appearance, (vii) rough surface appearance, and (viii) waviness of bead. The total range of bead penetration for AA6061 aluminum alloy was between 2.310 mm and 3.202 mm with an average bead penetration of 2.814 mm. Spatter defect was formed on the top surface of most welded joints in C-80 steel. The total range of bead penetration in C-80 steel was between 2.72 mm and 3.27 mm with an average bead penetration of 3.03 mm. All welding joints produced in C-80 steel contained an incomplete penetration. The spatter defect was more likely to occur during welding of CK45 steel at a low or moderate welding current (100 A and 110 A). The total range of bead penetration in CK45 steel was between 2.437 mm and 3.320 mm with an average bead penetration of 2.937 mm. Other than the joint produced at 100 A, 23 V, and 82 cm/min, an excessive penetration was observed in all other joints.

References

1. A.SH. Hasan, O.M. Ali, and A.M. Alsaffawi, Effect of welding current on weldments properties in MIG and TIG welding, *International Journal of Engineering & Technology*, 7 (2018) 192-197. 10.14419/ijet.v7i4.37.24099
2. D. Zhao, K. Zhao, D. Ren, and X.L. Guo, Ultrasonic welding of magnesium–titanium dissimilar metals: A study on influences of welding parameters on mechanical property by experimentation and artificial neural network, *Journal of Manufacturing Science and Engineering*, 139 (2017). 10.1115/1.4035539
3. L. Huang, D. Wu, X. Hua, S. Liu, Z. Jiang, F. Li, H. Wang, and S. Shi, Effect of the welding direction on the microstructural characterization in fiber laser-GMAW hybrid welding of 5083 aluminum alloy, *Journal of Manufacturing Processes*, 31 (2018) 514-522. 10.1016/j.jmapro.2017.12.010
4. M. Habibi, R. Hashemi, M. Fallah Tafti and A. Assempour, Experimental investigation of mechanical properties, formability and forming limit diagrams for tailor-welded blanks produced by friction stir welding, *Journal of Manufacturing Processes*, 31 (2018) 310-323. 10.1016/j.jmapro.2017.11.009
5. J. Yang, Z. Yu, Y. Li, H. Zhang and N. Zhou, Laser welding/brazing of 5182 aluminum alloy to ZEK100 magnesium alloy using a nickel interlayer, *Science and Technology of Welding and Joining*, 23 (2018) 543-550. 10.1080/13621718.2018.1425182
6. V. Kumar, M. Hussain, M. Shahid Raza, A. Kumar Das and N.K. Singh, Fiber laser welding of thin nickel sheets in air and water medium, *Arabian Journal for Science and Engineering*, 42 (2017) 1765-1773. 10.1007/s13369-016-2305-1
7. K. Krasnowski, Experimental study of FSW T-joints of EN-AW6082-T6 and their behaviour under static loads, *Arabian Journal for Science and Engineering*, 39 (2014) 9083-9092. 10.1007/s13369-014-1465-0
8. F. Kolahan and M. Heidari, A new approach for predicting and optimizing weld bead geometry in GMAW, World Academy of Science, Engineering and Technology, *International Journal of Mechanical, Aerospace, Industrial, Mechatronic and Manufacturing Engineering*, 2009.
9. M. Wêglowski, Y. Huang and Y.M. Zhang, Effect of welding current on metal transfer in GMAW, *Archives of Materials Science and Engineering*, 33 (2008) 49-56.

10. R.W. Messler Jr. (1999) Principles of Welding, Processes, Physics, Chemistry, and Metallurgy. New York, John Wiley & Sons, Chapter 3, ISBN: 9780471253761.
11. A.A. Nuraini, A.S. Zainal and M.A. Azmah Hanim, The effects of welding parameters on butt joints using robotic gas metal arc welding, *Journal of Mechanical Engineering and Science*, 6 (2014) 988-994. : http://dx.doi.org/10.15282/jmes.6.2014.26.0096
12. S. Ozcelik, K.L. Moore and D.S. Naidu, Modeling, Sensing, and Control of Gas Metal Arc Welding, Elsevier Science, Oxford (2003). ISBN: 9780080440668.
13. Y.-R. Wong and S.-F. Ling, An investigation of dynamical metal transfer in GMAW-Effects of argon shielding gas, *Journal of Materials Processing Technology*, 214 (2014) 106-111. https://doi.org/10.1016/j.jmatprotec.2013.08.003
14. U. Ersoy, S.J. Hu and E. Kannatey-Asibu, Observation of arc start instability and spatter generation in GMAW, *Welding Journal*, 87 (2008) 51-s-56-s.
15. I. Shareef and C. Martin, Effect of process parameters on weld spatter in robotic welding, *Procedia Manufacturing*, 48 (2020) 358-371. 10.1016/j.promfg.2020.05.058
16. M.J. Kang, Y. Kim, S. Ahn and S. Rhee, Spatter rate estimation in the short circuit transfer region of GMAW, *Welding Journal*, 82 (2003) 238-247.
17. J.H. Chen, Z.C. Sun and D. Fan, Study on the mechanism of spatter produced by basic welding electrodes, *Welding Journal*, 75 (1996) 311-s-316-s.
18. Welding handbook. Welding technology, 8th ed, vol. 1. American Welding Society, 550 NW LeJeune Road Miami, 1991.
19. Metals handbook. Welding, brazing and soldering, vol. 6. Ohio: ASM Int Metals Park, 1995.
20. M. Cerit, O. Kokumer and K. Genel, Stress concentration effects of undercut defect and reinforcement metal in butt welded joint, *Engineering Failure Analysis*, 17 (2010) 571-578. 10.1016/j.engfailanal.2009.10.010
21. M. Kurtulmuş and E. Doğan, The effects of undercut geometry on the static stress concentration factor of welds, *Emerging Materials Research*, 10 (2021) 1-6. https://doi.org/10.1680/jemmr.20.00100
22. Automated Welding Basics, Revolutionizing the world of welding, Technical Guide, www.keyence.com/
23. Welding Engineers, Efficient Welding Supply Solutions, Weld Defects, Reproduced from Kobelco Welding, Japan, https://weldingengineers.co.nz/
24. D.-Y. Kim, I. Hwang, G. Jeong, M. Kang, D. Kim, J. Seo, Y.-M. Kim, Effect of porosity on the fatigue behavior of gas metal arc welding lap fillet joint in GA 590 MPa steel sheets, *Metals*, 8 (2018) 241. https://doi.org/10.3390/met8040241
25. M. Harooni, B. Carlson, B.R. Strohmeier, R. Kovacevic, Pore formation mechanism and its mitigation in laser welding of AZ31B magnesium alloy in lap joint configuration, *Materials and Design*, 58 (2014) 265-276. https://doi.org/10.1016/j.matdes.2014.01.050
26. M. Harooni, F. Kong, B. Carlson and R. Kovacevic, Mitigation of pore generation in laser welding of magnesium alloy AZ31B in lap joint configuration, Proceedings of the ASME 2013 International Mechanical Engineering Congress & Exposition IMECE2012At: Houston, TX, USA, pp.919-927. 10.1115/IMECE2012-89073
27. M. Wahba, M. Mizutani, Y. Kawahito and S. Katayama, Laser welding of die-cast AZ91D magnesium alloy, *Materials and Design*, 33 (2012) 569-576. 10.1016/j.matdes.2011.05.016

28. K. Fahlström, J. Blackburn, L. Karlsson and L.-E. Svensson, Effect of laser welding parameters on porosity of welds in cast magnesium alloy AM50, *Modern Approaches on Material Science*, 1 (2018) 25-32. 10.32474/MAMS.2018.01.000106
29. Tips For Avoiding Common Flux-Cored Problems & Improving Your FCAW Welds, 2012, https://www.tregaskiss.com/
30. Ultrasonic inspection-differentiating excessive root penetration from root discontinuities, https://themysticwaves.com/
31. A. Omran, F.S. AL-Madani, M. Alazumi and S. Elkoum, Corrosion of 316 Ti motor-pump casings in deep water wells due to welding defects, NACE International Corrosion 2009 Conference & expo. ISBN: 09053 2009 CP.
32. A.R. Deshmukh, G. Venkatachalam, H. Divekar and M.R. Saraf, Effect of weld penetration on fatigue life, *Procedia Engineering*, 97 (2014) 783-789. 10.1016/j.proeng.2014.12.277
33. A.K. Dey, 15 most common welding defects, Causes and Remedies, https://whatispiping.com/
34. S. Kim, K. Jin, W. Sung and S. Nam, Effect of lack of penetration on the fatigue strength of high strength steel butt weld, *KSME Journal*, 8 (1994) 191-197. https://doi.org/10.1007/BF02953268
35. H.R. Ghazvinloo and A. Honarbakhsh-Raouf, Ductility of welded joints in CK45 carbon steel, *Materials Science*, 56 (2020) 359-362. https://doi.org/10.1007/s11003-020-00437-7
36. H.R. Ghazvinloo and A. Honarbakhsh-Raouf, Microstructure of the weld metal in CK45 carbon steel, *Materials Science*, 54 (2019) 748-752. https://doi.org/10.1007/s11003-019-00242-x
37. H.R. Ghazvinloo and A. Honarbakhsh-Raouf, Mechanical strength of the weld metal in CK45 carbon steel, *Materials Science*, 56 (2020) 210-213. https://doi.org/10.1007/s11003-020-00417-x
38. H.R. Ghazvinloo, Impact energy of weld metal in CK45 carbon steel, *Iranian Journal of Energy and Environment (IJEE)*, 11 (2020) 152-156. 10.5829/IJEE.2020.11.02.09